A modified phase coherence model for the non-linear *c*-axis *V*–*I* characteristics of highly anisotropic, high temperature superconductors

2003 J. Phys.: Condens. Matter 15 2351

(http://iopscience.iop.org/0953-8984/15/14/311)

INSTITUTE OF PHYSICS PUBLISHING JOURNAL OF PHYSICS: CONDENSED MATTER

J. Phys.: Condens. Matter **15** (2003) 2351–2362 PII: S0953-8984(03)38995-7

A modified phase coherence model for the non-linear *c*-axis V–I characteristics of highly anisotropic, high temperature superconductors

Sheng Luo[1,3], **Guohua Zhang**[1], **Saijun Huang**[1], **Yusheng He**[2], **Chunguang Li**[2] **and Xueqiang Zhang**[2]

[1] Department of Physics, University of Science and Technology Beijing, 30 Xue Yuan Lu, Beijing 100083, People's Republic of China
[2] National Laboratory for Superconductivity and Institute of Physics, Chinese Academy of Sciences, PO Box 2711, Beijing 100080, People's Republic of China

E-mail: sluo@sas.ustb.edu.cn, sluo2002@sina.com and yshe@cl.cryo.ac.cn

Received 3 July 2002, in final form 27 January 2003
Published 31 March 2003
Online at stacks.iop.org/JPhysCM/15/2351

Abstract

A modified Ambegaokar–Halperin thermal-fluctuation model has been developed to describe the *c*-axis V–I characteristics and low-current ohmic resistance of highly anisotropic superconductors in a magnetic field parallel to the *c*-axis. The model assumes loss of phase coherence across the CuO-planes associated with the correlated motion of pancake vortices in the liquid state. The predicted V–I characteristics in the current-induced transition from the superconducting to the resistive state are in good agreement with measurements on a 2212-BSCCO single crystal as a function of temperature and field, provided the effect of the interlayer capacitance is taken into account. The measurements are consistent with a flux pancake correlation length within the CuO-planes varying as $\xi_0/(T/T_0 - 1)^{\nu}$, where $\xi_0 = 1.57 \pm 0.08$ μm and $\nu = 0.50 \pm 0.01$. Our measurements imply a current-dependent interlayer resistance above and below T_c.

1. Introduction

There has been considerable interest in the *c*-axis conductivity of highly anisotropic, high temperature superconductor crystals such as 2212-BSCCO. There is convincing experimental evidence [1] that such crystals can be described by the Lawrence–Doniach model [2], as a series array of Josephson junctions formed between adjacent CuO planes. A number of authors have presented measurements of the temperature and field dependence of the *c*-axis resistance at low currents [1, 3–11]. A notable feature of all these measurements is the field-dependent

[3] Author to whom any correspondence should be addressed.

peak in resistivity, which arises from an increase in normal state resistivity on approaching T_c from above, and a broad transition to the zero resistance superconducting state.

Several theoretical models have been proposed to account for these measurements [12–18]. It was initially assumed that the increase in normal-state resistivity in the c-direction on decreasing temperature [12] reflected a quasi-semiconducting behaviour caused by electron localization within the CuO planes, with only weak temperature-dependent hopping probability between the planes. It has also been proposed that at least part of the increase in resistance is a consequence of superconducting fluctuations above T_c [13–18]. For example, Gray and Kim [16] successfully account for many of the observed features by a model in which superconducting fluctuations above T_c reduce the density of states of normal electrons, leading to a reduced quasi-particle tunnelling conductance and enhanced resistance between the layers. In contrast, superconducting fluctuations above T_c play little part in the tunnelling conductance, because of the lack of phase coherence of the fluctuations across adjacent planes. Alternatively, the anomalous behaviour may reflect a reduction of the normal electron density of states by the pre-formation of superconducting pairs above T_c, arising from a real gap in the electronic energy spectrum opening up along particular directions, as suggested by photon emission measurements [19–21].

In this paper, we will be primarily concerned with the effect of fluctuations on the current-induced resistive transition in a magnetic field below T_c. We assume a flux pancake liquid involving weak correlation of the pancakes between the planes. The c-axis superconducting tunnel current will then be determined by correlation of the superconducting order parameters between the planes, which in turn will depend on the correlated motion of flux pancakes both within and between the planes.

Above the melting transition, coherent tunnelling between the planes will be restricted to regions over which the flux pancakes are correlated across adjacent planes. Tunnelling across individual planes will then involve a parallel array of correlated tunnelling regions on a spatial scale determined by the correlation length of the mobile pancakes in the ab-planes. Very close to the superconducting transition the correlation length will be small and the Josephson coupling energy (proportional to the area of the coherently tunnelling region) will be comparable with thermal energies. This accounts for the large thermal broadening observed, which we describe in terms of a modified Ambegaokar–Halperin model [22]. However, as the temperature decreases towards a characteristic temperature T_0, the correlation length and Josephson coupling energy E_J increase, leading to the observed rapid decrease in thermal broadening. By comparing the functional form of the measured non-linear V–I characteristics with the predictions of such a model, assuming a correlation length varying as $\xi_{(T)} = \xi_0/(T/T_0 - 1)^{\nu}$, values for the correlation length ξ_0, T_0 and υ can be derived.

The above model differs from that of Bricenõ *et al* [6] who also considered tunnelling by a parallel array of Josephson junctions but assumed an effective length scale determined by $(\Phi_0/B)^{1/2}$. This fails to account for the rapid decrease in thermal broadening with decreasing temperature. Our model offers a physical justification for the empirical models previous assumed by Giura *et al* [9] and Kadowaki *et al* [10], who invoked the empirical Vogel–Fulcher equation [23, 24], in which activation is assumed to vary as $\exp(-A/(T - T_0))$. This is equivalent to our model if $\nu = 1/2$, as confirmed rather precisely from four-point measurements on a small single crystal of 2212-BSCCO.

Previous authors have confined their analysis and comparison with theory to the small current limit, where the V–I characteristics are ohmic. Here we fit our results over the whole range of currents required to induce a transition from the superconducting to normal state. We demonstrate the importance of including the interlayer capacitance into theoretical models, which has been ignored in previous analysis of the c-axis conductivity.

Another important parameter that has to be used in any comparison between theory and measurements is the effective parallel resistance R in the assumed RCSJ model. Gray and Kim assumed that R is given by the normal electron quasi-particle tunnelling current. For an s-state BCS superconductor the quasi-particle current would decrease very rapidly below T_c giving a rapid increase in R. A similar large increase in R at T_c would be expected for a d-state superconductor, but the conductivity might well remain finite at low temperatures as any impurity scattering would give a non-vanishing density of states of the quasi-particles near the nodes of the energy gap [25].

In contrast to the above models for R, we observe a limiting form of resistance at large currents both above and below T_c, which is close in value to the normal state values extrapolated from high temperatures. This observation is also consistent with observed hysteresis in the V–I characteristics when the McCumber parameter [26] $\beta > 1$, which again implies a fairly constant value of resistance on decreasing temperature. Indeed, at low temperatures, the hysteresis unexpectedly decreases, which is inconsistent with a rapidly decreasing quasi-particle conductance. In analysing our measurements, we have therefore adopted the pragmatic approach by identifying the shunt resistance as the resistance measured at large currents, which then allows us to fit our theoretical model to the measured characteristics over the whole of the current-induced transition from the superconducting to the resistive state below T_c. In practice, R may well depend not only on temperature and magnetic field but also on the current passing through the junctions, as indeed observed above T_c.

2. Theoretical model

Kleiner *et al* [1] have presented convincing evidence that 2212-BSCCO single crystals can be considered as a series array of Josephson junctions with superconducting properties described by the Lawrence–Doniach model [2]. In its simplest form, such a model assumes phase coherence across the whole area of the CuO planes. The V–I characteristics for currents flowing along the c-axis should therefore be given by the sum of the voltages across the Josephson junctions formed between each of the CuO planes. The influence of thermal fluctuations can be described by the AH model, though the effect of the finite inter-electrode capacitance must also be included.

The V–I characteristics for an individual junction, initially neglecting the inter-electrode capacitance, are given by [27]

$$V_0 = \frac{2}{\gamma} r_n(T) i_c(T) \frac{\exp(\pi\gamma\alpha) - 1}{\exp(\pi\gamma\alpha)} \Pi_1^{-1}, \tag{1}$$

where

$$\gamma = \frac{2E_J}{k_B T} = \frac{\hbar i_c(T)}{e k_B T}, \qquad \alpha = \frac{i(T)}{i_c(T)},$$

and

$$\Pi_1 = \int_0^{2\pi} \exp\left(-\frac{\gamma}{2}\alpha\varphi\right) I_0\left(\gamma \sin\frac{\varphi}{2}\right) \mathrm{d}\varphi. \tag{2}$$

These characteristics were numerically evaluated by Ambegaokar and Halperin [22] for a range of γ values (see also figure 6.22 of Barone and Paterno [29])

Inclusion of the interlayer capacitance results in increased phase slippage and therefore voltage V_1 across the junction. To first order in correction terms [27],

$$V_1 = V_0\left(1 + \beta\frac{\Pi_2}{\Pi_1}\right), \tag{3}$$

where β is the McCumber parameter [26],

$$\beta = \frac{2\pi i_c(T) r_n^2(T) c}{\phi_0}, \tag{4}$$

and

$$\Pi_2 = \int_0^{2\pi} \exp\left[\left(-\frac{\gamma}{2}\alpha\right)\varphi\right] I_1\left(\gamma \sin\frac{\varphi}{2}\right) \sin\frac{\varphi}{2}\, \mathrm{d}\varphi. \tag{5}$$

In the above expressions $i_c(T)$ is the intrinsic critical current, $r_n(T)$ the shunting resistance and c the capacitance of the individual RCSJ junctions, Φ_0 is the flux quantum, and I_0 and I_1 are modified Bessel functions. A single crystal can be considered as a series array of N such junctions. The voltage across the crystal for a given current will simply be N times the voltage across the individual junctions, $r_n(T) = R_n(T)/N$ and $c = NC$, where $R_n(T)$ and C are the normal state resistance and capacitance across opposite faces of the bulk crystal.

For an over-damped junction ($\beta \ll 1$) in the limit $i \ll i_c$, equation (1) reduces to $V = i r_n I o(\gamma/2)^{-2} \sim i r_n \gamma \mathrm{e}^{-\gamma}$. In the under-damped limit ($\beta \gg 1$) for small currents, $\Pi_2/\Pi_1 = \gamma/4$ for small γ and approaches unity for large γ.

Superconducting coherence across the relatively large area of crystals on which measurements are typically made ($\sim$0.01 mm^2) would result in a very large Josephson coupling energy E_J between adjacent sets of CuO_2 planes. Typical γ values ($\sim E_J/k_BT$) at temperatures only few degrees below T_c would exceed 1000 for observed critical current densities ($\sim$20 A cm^{-2}) along the c-direction. Such large γ values would imply a very sharp resistive transition to the normal state, inconsistent with the large thermal rounding observed.

The above model assumes phase coherence across the whole area of the CuO planes. However, the observed thermal broadening of the resistive transition in small field is far too large to be described by such a model. A much narrower transition would be expected if tunnelling occurred coherently across the whole area of the crystal because of the very large Josephson energy.

We therefore postulate that, above a characteristic temperature T_0, the superconducting phase is coherent only over a distance determined by the correlation length of vortex pancakes within the ab-planes, which is assumed to vary on approaching T_0 as $\xi_0/(T/T_0 - 1)^{\nu}$. The effective area, and hence Josephson energy, of each junction is therefore reduced by the factor $f = [\xi_0^2/(T/T_0 - 1)^{2\nu}]/A$, where A is the cross-sectional area of the bulk crystal. The reduced correlation length and hence reduced Josephson energy of the coherently tunnelling regions accounts for the enhanced thermal broadening between T_0 and T_c.

3. Experimental results

2212-BSCCO single crystals were grown by a large temperature gradient self-flux method. A large sample (typically 2 mm square and a few microns thick) was first cleaved from a parent crystal using a sharp scalpel. Gold was then sputtered on to one of the major faces using a 38 swg copper wire as a shadow mask to separate two contact areas for independent current and voltage contacts. Small-area samples bridging the contact areas were then cut from the parent crystal with a typical size of 50 $\times$ 100 μm. The small size was required to ensure that the aerial dimensions were less than Josephson penetration length, at least near T_c, so that the small-junction expressions used for tunnelling are justified. The sample was bonded with conducting epoxy to a glass substrate with two sputtered gold contacts areas. Electrical contacts were made with 25 μm gold wires using silver epoxy (type-Du Pont 6838). The mounted crystal was then baked at 350 °C in flowing air for 20 min to stabilize the electrical

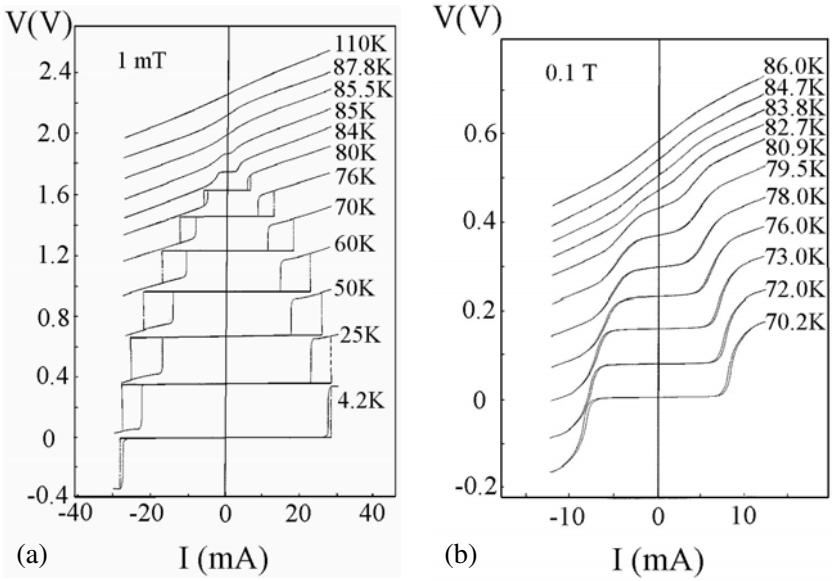

Figure 1. V–I characteristics along the c-axis of 2212-BSCCO single crystals at temperatures indicated in magnetic fields of: (a) 1 mT and (b) 0.1 T.

contacts, which had typical resistances of a few ohms. The sample was mounted in a continuous flow cryostat enabling measurements to be made over the full superconducting temperature range in fields parallel to the c-direction up to 0.1 T.

We present four-point measurements on a single 2212-BSCCO crystal ($50 \times 130 \times 1\ \mu$m) for which a full set of V–I characteristics as a function of temperature and field was made. Qualitatively similar characteristics were obtained for a number of other crystals investigated, but the fragility of the electrical contacts on exposure to repeated thermal cycling resulted in only one full set of measurements being made over a complete set temperatures, fields and currents.

4. Measurements

Typical four-point V–I characteristics in fields of 1 mT and 0.1 T are shown in figures 1(a) and (b), respectively. We first note marked deviations from ohmic behaviour well above T_c, consistent with earlier two-point measurements on similar 2212-BSCCO crystals [28]. The increased slope in the V–I characteristics at small currents above T_c leads to a significant increase in resistance on approaching T_c from above, see figure 1, similar to measurements reported by previous authors [6, 9, 10]. In our crystals, the increase in resistance on approaching T_c is intimately related to the observed non-linearity in the V–I characteristics at small currents (μA). At higher currents (mA) the resistance becomes ohmic and continues to decrease slightly with temperature in the resistive state both above and below T_c, as indicated in figure 2.

At 1 mT a critical current is first observed at ∼86 K, with a transition to the normal state which is appreciably broadened by thermal fluctuations. Hysteresis in the V–I characteristics sets in at around 83 K, increasing in width to a maximum at ∼50 K but decreasing at lower temperatures. At larger fields, figure 1(b), the transition region is significantly broadened at all temperatures, with a reduced critical current and hysteresis. In this paper we confine

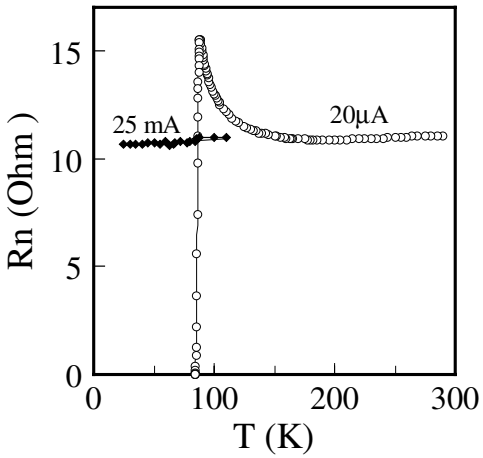

Figure 2. The temperature dependence of the *c*-axis resistance of a 2212-BSCCO single crystal sample in 1 mT magnetic field, where the open circles represent small current (20 μA) results and the solid diamonds show the large current (25 mA) results.

our discussion to the V–I characteristics in increasing current for temperatures above the irreversibility line and interpret our measurements in terms of the theoretical model developed in section 2.

5. Interpretation of measurements

If we assume coherent tunnelling across the whole area of the crystal planes, the value of γ at 85 K estimated from the *measured* critical current would be >600. Such a value would lead to an extremely sharp resistive transition (see figure 1 of [22] or figure 6.22 of [29]), whereas the observed transition is appreciably rounded (figure 1(a)), implying a much smaller effective γ value. Furthermore, the thermal broadening decreases very rapidly on approaching a characteristic temperature T_0, which implies a rapid increase in effective γ value with decreasing temperature. Below this temperature T_0, we always observe a very sharp current-induced transition from superconducting to resistive state.

As described above, the large thermal broadening can be explained if we assume an effective γ value reduced by the factor $f = [\xi_0/(T/T_0 - 1)^{\nu}]^2/A$. By fitting predicted V–I characteristics to the measured characteristics, we derive values for γ and hence determine the values of T_0, ν and the magnitude and temperature dependence of the correlation length $\xi(T)$.

In comparing with theoretical models, we have assumed that R_n is given by the extrapolated value of the *measured* resistance at large currents, which only changes slightly with temperature over the temperature range of interest (figure 2). The interlayer capacitance can be estimated from the onset of hysteresis in the V–I characteristics, which occurs when $\beta = 1$. Using the measured critical current to estimate i_c gives $c \sim 0.2$ F m^{-2}, corresponding to an estimated dielectric constant for the crystal $\sim$30. This value is comparable with what is often assumed in measurements of the Josephson plasma frequency at microwave frequencies [30, 31], though the dielectric constant may well depend on the state of oxygenation and hence be sample dependent.

Assuming that the V–I characteristics can be described by a series–parallel array of independent Josephson junctions, as described in section 2, the current flowing through

individual junctions, $i(T)$, is expected to vary as

$$i(T) = fI(T) = \xi_0^2\left[\frac{T_0}{(T - T_0)}\right]^{2\nu}\frac{I(T)}{A}, \tag{6}$$

with the shunting resistance and capacitance of the individual junctions given by $r_n(T) = R_n(T)/fN$ and $c = CNf$. The voltage across the sample is then given by equation (3),

$$V_1 = V_0\left(1 + \beta\frac{\Pi_2}{\Pi_1}\right),$$

where V_0, Π_1 and Π_2 are now given by equations (1), (2) and (5), with

$$\alpha(T) = \frac{i(T)}{i_c(T)} = \frac{I(T)}{I_c(T)}, \tag{7}$$

$$\gamma(T) = \frac{\hbar i_c(T)}{ek_BT} = \frac{\hbar I_c(T)}{ek_BT}\frac{\xi_0^2}{A}\left(\frac{T_0}{(T - T_0)}\right)^{2\nu}, \tag{8}$$

and

$$\beta = \frac{2\pi i_c(T)r_n^2 c}{\Phi_0} = \frac{2\pi I_c(T)R_N^2 C}{N\Phi_0}, \tag{9}$$

where $i_c(T)$ and $I_c(T)$ are the intrinsic critical currents in the absence of thermal fluctuations for the individual junctions and for the whole crystal respectively.

In figures 3(a), (b) and (c) we show representative V–I characteristics over a range of temperatures at fields of 1 mT, 0.04 and 0.1 T, respectively. Superimposed on this data, we have plotted theoretical curves calculated from equation (3) using the measured large current $R_n(T)$ in the range 8–11 Ω, $N = 650$, and $C = 2.0 \times 10^{-12}$ F. These values were then used in determining $\gamma(T)$ and $I_c(T)$, by fitting the V–I characteristics calculated from equation (3) to the measured data.

Derived values of $I_c(T)$ and $\gamma(T)$ are plotted in figures 4 and 5. Note that the intrinsic $I_c(T)$ initially increases linearly with T below T_c for all fields. In figure 6, we have re-plotted the fitted parameters in the form $\frac{\gamma(T)}{I_c(T)} = \frac{\hbar}{ek_BT}\frac{\xi_0^2}{A_s}\left(\frac{T_0}{T-T_0}\right)^{2\nu}$. This enables us to extract values of T_0 and ν from the observed temperature dependence. We obtain $\xi_0 = 1.57 \pm 0.03$ μm and $\nu = 0.50 \pm 0.01$ for all three fields, with the characteristic temperatures, T_0, of 79.8, 72.0 and 67.0 K in fields of 1 mT, 0.04 and 0.1 T respectively.

Also included in figures 3(a)–(c) are theoretical V–I characteristics calculated neglecting both thermal fluctuations and interlayer capacitance (dotted curves) and characteristics including thermal fluctuations but ignoring capacitance (dashed curves). Note the significant increase in voltage across the crystal when the interlayer capacitance is included, which is also required to account for the functional form of the V–I characteristics.

At small currents, the AH-model, modified to include the effect of interlayer capacitance, predicts a small current ohmic resistance

$$R = V/I = R_n\left[I_0\left(\frac{\gamma}{2}\right)\right]^{-1}\left(1 + \beta\frac{\Pi_2}{\Pi_1}\right). \tag{10}$$

Note that the interlayer capacitance significantly enhances the resistance, but was ignored in earlier models for the c-axis resistance [4, 7, 8].

In figure 7 the low current (20 μA) resistance is plotted on a logarithmic scale as a function of temperature for the three fields investigated. The solid curve represents the predictions of equation (10) in the small current limit assuming the same parameters used to fit the V–I characteristics in the current-induced superconducting to normal state regime, as indicated in figures 3(a)–(c). The dashed curves are values predicted if the interlayer capacitance had been neglected (i.e. equation (1)). Even when the capacitance is included, the measured resistance is somewhat larger than predicted.

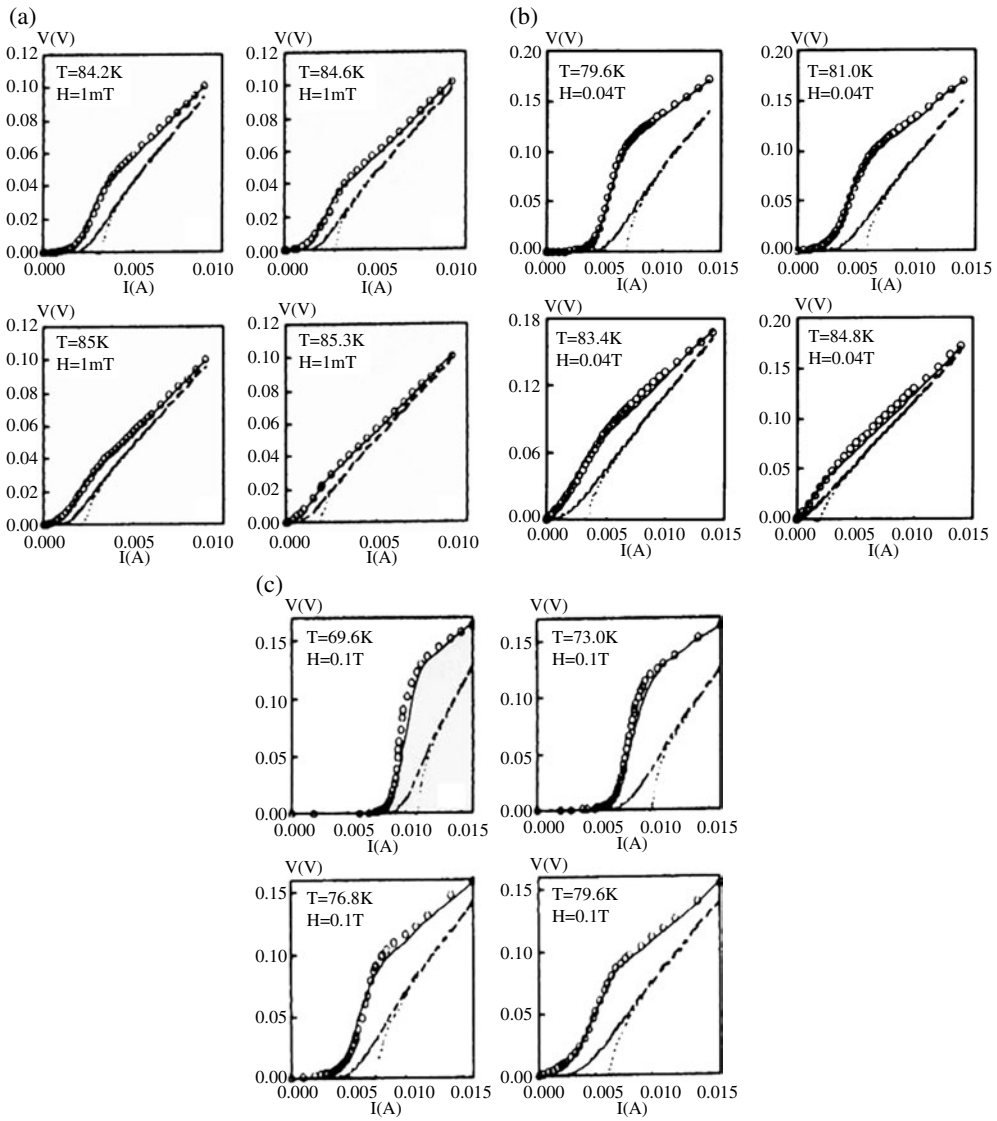

Figure 3. Representative V–I characteristics along the c-axis of 2212-BSCCO single crystals measured over a range of temperatures at fields of (a) 1 mT (b) 0.04 T and (c) 0.1 T, shown as solid circles. Calculated curves from three different models are also shown: the solid curve represent the fitted results from equation (3); the dashed curve is from the original A–H model neglecting capacitance (equation (1)); the dotted curve is the RCSJ model which neglects both capacitance and thermal fluctuations. The parameters used for all three curves are the same and are referred to in the text.

The larger value of resistance measured at low currents might be explained if the shunting resistance R is current dependent with a larger value at small currents, as is indeed observed above T_c. The finite quasi-particle current between the planes could lead to a non-equilibrium depression of the order parameter in the individual CuO planes, which would then reduce i_c and γ leading to a larger thermally activated resistance.

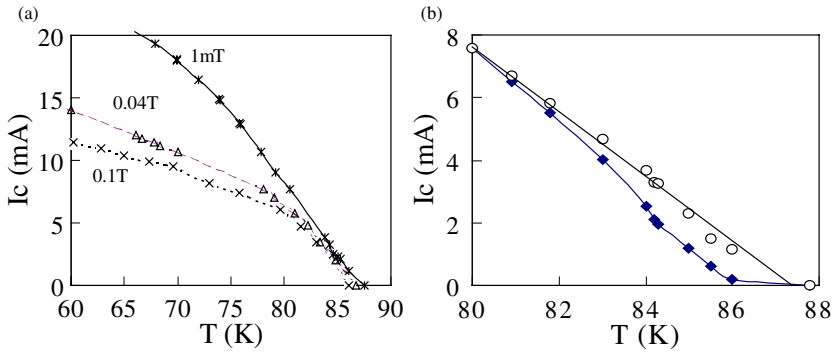

Figure 4. (a) Temperature dependence of the intrinsic critical current $I_c(T)$ at fields of 1 mT, 0.04 and 0.1 T, derived from best fitting of V–I characteristics. (b) Comparison between apparent critical currents obtained from direct measurement (solid diamonds) and the intrinsic critical currents derived from best fittings at 1 mT (circles).

(This figure is in colour only in the electronic version)

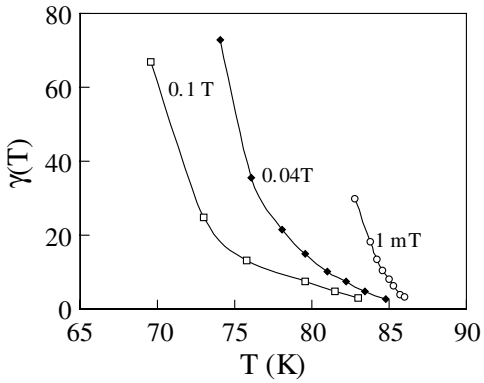

Figure 5. Temperature dependence of the parameter $\gamma(T)$ at fields of 1 mT, 0.04 and 0.1 T, derived from best fitting of V–I characteristics.

Another possibility for the increased low temperature resistance would be sample inhomogeneity. Any layer of the crystal having a slightly depressed value of I_c would contribute a significantly enhanced resistivity at low temperatures. The agreement between theory and experiment can be improved significantly, for example, if we assume that I_c in a quarter of the layers is depressed by $\sim$20%. Such a variation in I_c is consistent with the appearance of early critical current transitions at low temperatures, and variations in critical currents between individual CuO layers in measurements on mesa structures [32]. Such variations in critical current could easily arise from local inhomogeneities in oxygen concentration, microstructural defects (vacancies, dislocations, slip planes, etc) or from damage near the surface of the crystal associated with the electrical contact regions. Furthermore, it must be emphasized that equation (10) only includes first-order corrections for the influence of capacitance, so that exact agreement between theory and experiment is not expected.

Although our model provides an excellent description of the non-linear c-axis V–I characteristics of 2212-BSCCO in the current-induced transition region below T_c, there are a number of features that require further investigation. In particular, there remains the problem

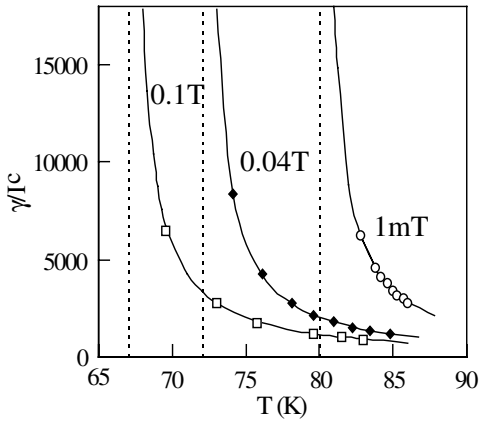

Figure 6. Fitted values in the form of $\gamma(T)/I_c(T)$ are shown as function of temperature in three magnetic fields. The symbols represent values derived from V–I curve fitting and the solid curves are the best fit to the relation of $\xi = \xi_0/(T/T_0 - 1)^{\nu}$. Fitted values were $\xi_0 = 1.57 \pm 0.08$ μm and $\nu = 0.50 \pm 0.01$ independent of field, with values of $T_0 = 79.8$, 72.1 and 67.1 K for 1, 40 and 100 mT respectively.

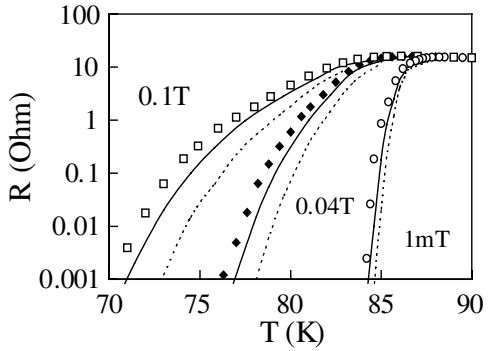

Figure 7. Temperature dependence of the c-axis resistance of a 2212-BSCCO single crystal sample measured at 20 μA (shown as symbols) for the three fields as indicated. The solid curves represent the predicted values by equation (10), whereas the dotted curves show the predicted values neglecting capacitance.

of the appropriate value of R to be used in any analysis. Any complete model for the non-linear V–I characteristics must also describe the behaviour above as well as below T_c.

An important observation is that the resistance in the phase-slip regime at large currents approaches the extrapolated normal state value both above and below T_c. This is inconsistent with an intrinsic quasi-particle resistance in either s- or d-state models, where the shunting resistance would be expected to rise appreciably below T_c. Our observations are consistent with a shunt resistance R, which depends weakly on field and temperature but also depends on current. This may reflect an intrinsic property of the interlayer tunnel junctions in these highly anisotropic superconductors. However, it is also possible that the shunt resistance is a non-intrinsic property, even in high quality single crystals, produced by 'micro-shorts' between the individual CuO planes, possibly involving electronic defects associated with microscopic variations in oxygen or compositional stoichiometry.

Finally it is worth pointing out that the physical meaning of the characteristic temperature T_0 is a very important but yet unsolved question. It is well known that the Vogel–Fulcher

law, from which T_0 is derived, remains a pure fitting formula, even though it describes the viscosity over a range of ten decades and more. Generally speaking there is no microscopic physical meaning for it. For our particular case, however, there are some hints to incorporate this fitted temperature to the vortex liquid–glass transition temperature T_g. Independent measurements on crystals from the same growth batch of the sample used confirm that the above T_0 values are within a degree or so of the irreversibility temperature determined magnetically. Furthermore, a recent attempt to scale the c-axis V–I characteristics shown in this paper has been quite successful. Preliminary results (to be published elsewhere) show that after scaling the decreasing current branches of the V–I curves measured at different temperatures collapse nicely onto two curves, with positive ($T > T_g$) and negative ($T < T_g$) curvature respectively. The extracted scaling parameter, T_g, is quite close to the characteristic temperature T_0 derived from Vogel–Fulcher law. A detailed study is being carried out in this direction and a deeper understanding of the physical meaning of T_0 is, of course, still an open and important topic for further study.

6. Conclusions

We have shown that the c-axis V–I characteristics and resistance of a 2212-BSCCO single crystal can be described by a modified Ambegaokar–Halperin model. We propose a phase coherence model involving a loss of phase coherence of the superconducting order parameter within individual CuO_2 planes determined by the flux lattice correlation length $\xi_0/(T/T_0-1)^{\nu}$ in the liquid state. We obtain values for $\nu = 0.50 \pm 0.01$ and $\xi_0 = 1.57\ \mu$m in fields up to 0.1 T. This model successfully accounts for the rapid change in the thermal rounding below T_c on approaching the fitted characteristic temperature T_0. To account for the functional form of the V–I characteristics, we show that it is essential to include the affect of interlayer capacitance. We also demonstrate that the intrinsic I_c varies linearly with temperature close to T_c.

A major unresolved problem relates to the value that should be used for the parallel resistance R. To describe our measurements we use the measured value of R at large currents both above and below T_c, but this fails to account for the observed increase in R and non-linear V–I characteristics above T_c. Further theoretical and experimental studies of the c-axis conductance both above and below T_c are clearly required.

Acknowledgments

We are grateful to Professor Colin Gough of Birmingham University for encouraging discussions. Part of the experimental work was conducted in his laboratory. Support from EPSRC (UK), NSFC (China), the Chinese Academy of Sciences and the Royal Society (UK) is also acknowledged.

References

[1] Kleiner R, Steinmeyer F, Kunkel G and Mueller P 1992 *Phys. Rev. Lett.* **68** 2394
Kleiner R and Mueller P 1994 *Phys. Rev.* B **49** 1327
[2] Lawrence W E and Doniach S 1971 *Proc. 12th Int. Conf. of Low Temperature Physics* ed E Kanda (Kyoto: Academic) p 361
[3] Kitazawa K, Kambe S, Naito M, Tanaka I and Kojima H 1989 *Japan. J. Appl. Phys.* **28** L555 A
Kambe S, Naito M, Kitazawa K, Tanaka I and Kojima H 1989 *Physica* C **160** 243
[4] Latyshev Y I and Volkov A F 1991 *Physica* C **182** 47
[5] Busch R, Ries G, Werthner H, Kreiselmeyer G and Saemann-Ischenko G 1992 *Phys. Rev. Lett.* **69** 522
[6] Bricenõ G, Crommie M F and Zetll A 1993 *Physica* C **204** 389

Bricenõ G, Crommie M F and Zetll A 1991 *Phys. Rev. Lett.* **66** 2164
[7] Balestrino G, Marinelli M, Milani E, Varlamov A A and Yu L 1993 *Phys. Rev.* B **47** 6037
[8] Cho J H, Maley M P, Fleshler S, Lacerda A and Bulaevskii L N 1994 *Phys. Rev.* B **50** 6493
[9] Giura M, Sarti S, Silva E, Fastampa R, Murtas F, Marcon R, Adrian H and Wagner P 1994 *Phys. Rev.* B **50** 12920
Fastampa R, Giura M, Marcon R, Sarti S and Silva E 1993 *Supercond. Sci. Technol.* **6** 53
Giura M, Marcon R, Silva E and Fastampa R 1992 *Phys. Rev.* B **46** 5753
[10] Kadowaki K, Yuan S L, Kishio K, Kimura T and Kitazawa K 1994 *Phys. Rev.* B **50** 7230
Kadowaki K, Yuan S L and Kitazawa K 1994 *Supercond. Sci. Technol.* **7** 519
[11] Hashimoto K, Nakao K, Kado H and Koshizuka N 1996 *Phys. Rev.* B **53** 892
[12] Martin S, Fiory A T, Fleming R M, Schneemeyer L F and Waszczak J V 1988 *Phys. Rev. Lett.* **60** 2194
[13] Ioffe L B, Larkin A I, Varlamov A A and Yu L 1993 *Phys. Rev.* B **47** 8936
[14] Balestrino G, Marinelli M, Milani E, Varlamov A A and Yu L 1993 *Phys. Rev.* B **47** 6037
[15] Dorin V V, Klemm R A, Varlamov A A, Buzdin A I and Livanov D V 1993 *Phys. Rev.* B **48** 12951
[16] Gray K E and Kim D H 1993 *Phys. Rev. Lett.* **70** 1693
Kim D H, Gray K E and Kang J H 1992 *Phys. Rev.* B **45** 7563
Kim D H, Gray K E, Kampwirth R T, Smith J C, Richeson D S, Marks T J, Kang J H, Talvacchio J and Eddy M 1991 *Physica* C **177** 431
[17] Volkov A F 1993 *Solid State Commun.* **88** 715
[18] Koshelev A E 1996 *Phys. Rev. Lett.* **76** 1340
[19] Loeser A G, Shen Z-X and Dessau D S 1996 *Physica* C **263** 208
[20] Marshall D S, Dessau D S, Loeser A G, Park C-H, Matsusra A Y, Eckstein J N, Bozovic I, Fournier P, Kapitulnik A, Spicer W E and Shen Z-X 1996 *Phys. Rev. Lett.* **76** 4841
[21] Ding H, Yokoya T, Campuzano J C, Takahashi T, Randeria M, Norman M R, Mochiku T, Kadowaki K and Giapintzakis J 1996 *Nature* **382** 51
[22] Ambegaokar V and Halperin B I 1969 *Phys. Rev. Lett.* **22** 1364
[23] Vogel H Z 1921 *Physica* **22** 645
[24] Fulcher G S 1925 *J. Am. Ceram. Soc.* **6** 339
[25] Lee P A 1993 *Phys. Rev. Lett.* **71** 1887
[26] McCumber D E 1968 *J. Appl. Phys.* **39** 2503
[27] Lee P A 1971 *J. Appl. Phys.* **42** 325
[28] Luo S, Yang G and Gough C E 1995 *Phys. Rev.* B **51** 6655
[29] Barone A and Paterno G 1982 *Physics and Applications of the Josephson Junction Effect* (New York: Wiley–Interscience)
[30] Tsui O K C, Ong N P and Peterson J B 1996 *Phys. Rev. Lett.* **76** 819
Tsui O K C, Ong N P, Matsuda Y, Yan Y F and Peterson J B 1994 *Phys. Rev. Lett.* **73** 724
[31] Matsuda Y, Gaifullin M B, Kumagai K, Kadowaki K and Mochiku T 1995 *Phys. Rev. Lett.* **75** 4512
[32] Yurgens A, Winkler D, Zhang Y M, Zavaritsky N and Claeson T 1994 *Physica* C **235–240** 3269